Simulation of High Pressure Liquid Hydrogen Releases

Houf, W.G.[1] and Winters, W.S.[1]
[1]Sandia National Laboratories, Livermore, CA 94551-0969, USA, will@sandia.gov

ABSTRACT

Sandia National Laboratories is working with stakeholders to develop scientific data for use by standards development organizations to create hydrogen codes and standards for the safe use of liquid hydrogen. Knowledge of the concentration field and flammability envelope for high-pressure hydrogen leaks is an issue of importance for the safe use of liquid hydrogen. Sandia National Laboratories is engaged in an experimental and analytical program to characterize and predict the behavior of liquid hydrogen releases. This paper presents a model for computing hydrogen dilution distances for cold hydrogen releases. Model validation is presented for leaks of room temperature and 80K high-pressure hydrogen gas. The model accounts for a series of transitions that occurs from a stagnate location in the tank to a point in the leak jet where the concentration of hydrogen in air at the jet centerline has dropped to 4% by volume. The leaking hydrogen is assumed to be a simple compressible substance with thermodynamic equilibrium between hydrogen vapor, hydrogen liquid and air. For the multiphase portions of the jet near the leak location the REFPROP equation of state models developed by NIST are used to account for the thermodynamics. Further downstream, the jet develops into an atmospheric gas jet where the thermodynamics are described as a mixture of ideal gases (hydrogen-air mixture). Simulations are presented for dilution distances in under-expanded high-pressure leaks from the saturated vapor and saturated liquid portions of a liquid hydrogen storage tank at 10.34 barg (150 psig).

1.0 INTRODUCTION

The model for a high-momentum leaking hydrogen jet is shown in Fig. 1. The leak stream is assumed to be divided into a sequential series of "zones" that describe the physics of a high-momentum hydrogen jet as it is diluted with air in the atmosphere. The zones shown in Fig. 1 are not to scale either in the axial coordinate, *s* or the radial coordinate, *r*. The Zones 0, 1, 2, and 3 are in fact negligibly small compared to Zone 4 which represents the largest portion of the jet. The coordinate *s* represents the location along the jet centerline relative to the leak exit plane. The jet centerline may curve upward or downward due to buoyancy. The relationship between coordinates *s* and *r* and the global Cartesian coordinates *x, y*, and *z* is shown in Fig. 2. The hydrogen leak jet is assumed to be a steady-state leak from an infinite source of hydrogen. The state of the hydrogen in the storage vessel be saturated hydrogen vapor, saturated hydrogen liquid, subcooled liquid hydrogen, or superheated hydrogen gas and is assumed to be at low or zero velocity. Both air and hydrogen are assumed to be simple compressible substances in thermodynamic equilibrium regardless of whether they exist in multiple liquid-vapor phases or in a mixture of gases.

Important thermodynamic states or "stations" in the flow stream are identified with the numbers 0-5 along the centerline of the jet in Fig. 1. Downstream of Station 3 *(i.e.,* Zones 3 and 4), the stream of hydrogen and entrained air is modeled as a mixture of ideal gases at atmospheric pressure. Upstream of Station 3, *i.e.* Zones 0, 1, and 2, the thermodynamics are complicated and require equations of state that account for multiple phases (liquid, vapor and possible solid phases) and non-ideal hydrogen and air conditions. For these zones REFPROP [1] a program that utilizes thermodynamic models developed by NIST is used to calculate the state of leaking hydrogen and the state of hydrogen-air

---

[1]Sandia is a multiprogram laboratory operated by Sandia Corporation, a Lockheed Martin Company, for the United States Department of Energy's National Nuclear Security Administration under Contract DE-AC04-94-AL85000.

mixtures. In the following sections, modeling assumptions and equations are presented for each zone in the leak jet.

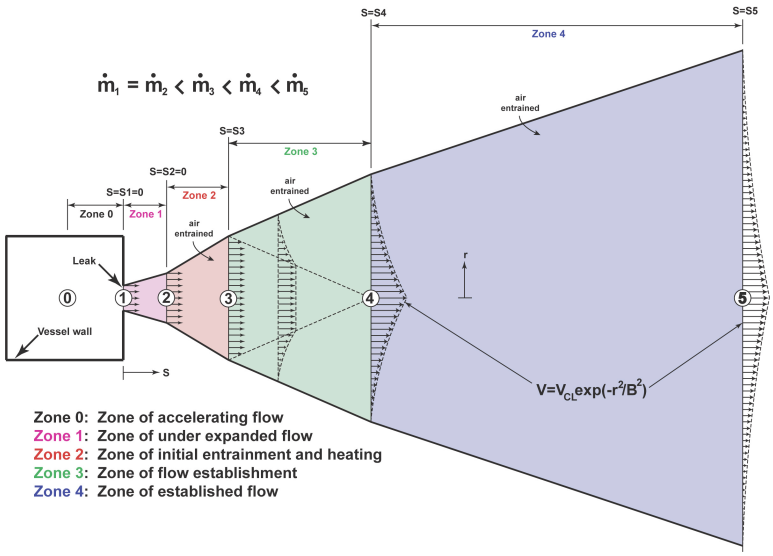

Figure 1. Model for high-momentum hydrogen leak.

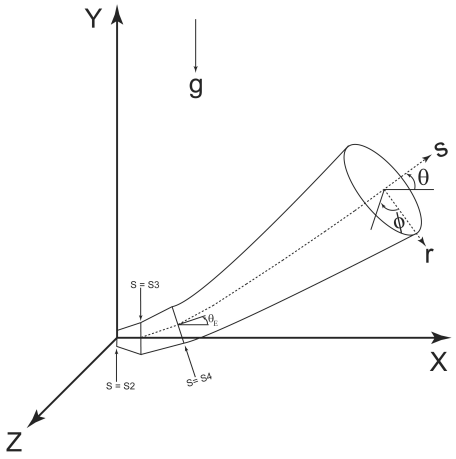

Figure 2. Leak jet coordinate system.

2.0 MODEL DESCRIPTION

2.1 Zone 0 – Zone of accelerating flow

For high-momentum leaks, it is assumed that the leak area is open to the atmosphere and there is negligible frictional pressure drop in the flow path between the stored hydrogen at Station 0 and the leak plane at Station 1. We assume that the thermodynamic state at Station 0 is known and the velocity at that location (a short distance from the leak plane) is very small. Potential energy changes and heat transfer from the accelerating stream to the surroundings are assumed to be negligibly small. The equations required to determine the state and mass flow rate of hydrogen at Station 1 are determined from the energy equation and the observation the acceleration of flow from rest to the leak plane is isentropic, *i.e.*,

$$h_1 + \frac{1}{2}V_1^2 = h_0 \tag{1}$$

$$s_1 = s_0 \tag{2}$$

Except for the rare case where hydrogen is stored as a gas at a pressure less than 0.1925MPa (1.9 atm), the flow at Station 1 will be choked. Nevertheless, the procedure used to determine the velocity and state at Station 1 must take into account the possibility of both choked and unchoked flow. This procedure makes use of Equations (1) and (2) and numerous calls to the REFPROP subroutines to calculate trial states at Station 1. Enthalpy (h_1), density (ρ_1), temperature (T_1), and quality (Q_1) at Station 1 are computed from two independent thermodynamic properties, namely the entropy as given by Eq. (2) and a trial pressure, P_1 as follows:

$$h_1 = h(P_1, s_1) \tag{3}$$

$$\rho_1 = \rho(P_1, s_1) \tag{4}$$

$$T_1 = T(P_1, s_1) \tag{5}$$

$$Q_1 = Q(P_1, s_1) \tag{6}$$

where the functions on the right-hand side are intended to represent returned thermodynamic properties from REFPROP subroutine calls. Note that Equation (6), the equation for quality, only has relevance for two phase flow at Station 1.

In addition to the properties determined from Eqs. (3)-(6), the computational procedure for Zone 0 requires the sound speed (C_1) for Station 1. For cases where the hydrogen at Station 1 is either a subcooled liquid or a superheated gas, REFPROP is capable of returning the sound speed using an appropriate subroutine call, *i.e.*

$$C_1 = C(P_1, s_1)\,. \tag{7}$$

For these cases, REFPROP determines the sound speed from the classical thermodynamic definition given by

$$C = \sqrt{\left(\frac{\partial P}{\partial \rho}\right)_s}\,. \tag{8}$$

However, if the state at Station 1 is a two-phase mixture (liquid and vapor), REFPROP returns no values for sound speed. This is primarily due the fact that computational methods for determining sound speed for liquid-vapor mixtures are somewhat controversial and cannot be accomplished using the standard definition expressed by Eq. (8). Of course it is always possible make a series of calls to REFPROP for the purpose of carrying out a numerical differentiation as indicated by Eq. (8), however, doing so will not yield values for the sound speed of saturated liquid as the quality approaches zero nor the sound speed of saturated vapor as the quality approaches 1.

The subject of sound speed determination for liquid-vapor mixtures has been addressed extensively in the literature see *e.g.* references [2-4]. In the present work we utilize the method of Chung et al. [5] for those cases where the state at Station 1 is two-phased. We chose this method because it is relatively easy to implement and Chung *et al*. have provided experimental validation for bubbly two-phase flow.

The procedure for computing the state at Station 1 is summarized below. The pressure and entropy at Station 1 are initially set to those at Station 0. P_1 is then decreased by a vanishingly small pressure decrement. A value of ΔP equal to $\left(P_0 - P_{ATM}\right)/1000$ was found to produce sufficiently accurate results. The properties and sound speed at Station 1 are then computed from appropriate REFPROP calls and the applicable sound speed model. The velocity at Station 1 is then computed from the energy equation (Eq. (1)). If the computed velocity exceeds the sound speed, the calculations are stopped and the flow is choked. If not, a test is made to see if the value of P_1 is less than or equal to

atmospheric pressure. If it is, calculations are stopped and the flow is unchoked. Failing the velocity and pressure tests, the trial value of P_1 is decremented by ΔP and the process is repeated.

2.2 Zone 1 – Zone of Under Expanded Flow

For the rare case when the flow is not choked at Station 1, the properties, flow area and velocity at Station 2 are set equal to their corresponding values at Station 1. For all other cases, the flow in Zone 1 is that of an under expanded jet and a source model must be used to determine the conditions at Station 2. The source model is intended to extrapolate conditions from the leak plane where the pressure is relatively high and the flow area is equal to the leak area to an "equivalent source" where the pressure is atmospheric and the flow area is somewhat larger than the leak area. Birch [6] and others have developed source models that are loosely based on one-dimensional flow conservation equations. These models generally produce nonphysical flow conditions at the source in the sense that the source Mach numbers are almost always transonic (Mach numbers greater than unity). Nonetheless these models appear to be successful in establishing boundary conditions for atmospheric turbulent entrainment models thus enabling them to be used to predict velocity and concentration fall-off in the far field jet.

In the present work, we utilize the source model of Xiao *et al.* [7] and Yuceil and Ottugen [8] to determine conditions at Station 2. The following assumptions are made when applying this model: (1) no air is entrained into Zone 1; (2) the pressure at Station 2 is equal to the atmospheric pressure ($P_2 = P_{ATM}$); (3) the flow is frictionless; (4) changes in potential energy are negligible; (5) buoyancy of the jet relative to the ambient is neglected; (6) heat transfer to the ambient is neglected; and (6) flow in Zone 1 is steady and one-dimensional.

Applying these assumptions yields the following conservation equations for Zone 1:

Continuity: $$\dot{m}_2 = \dot{m}_1 \tag{9}$$

Momentum: $$\left(\frac{\pi D_1^2}{4}\right) P_1 + \dot{m}_1 V_1 = \left(\frac{\pi D_1^2}{4}\right) P_{ATM} + \dot{m}_1 V_2 \tag{10}$$

Energy: $$h_1 + \frac{1}{2} V_1^2 = h_2 + \frac{1}{2} V_2^2 \tag{11}$$

The process of determining the source velocity, thermodynamic properties, and jet diameter at Station 2 is straightforward since the state and mass flow rate at Station 1 are known. Initially the velocity, V_2, at Station 2 is computed from Eq. (10) and the enthalpy, h_2, at Station 2 is computed from Eq. (11). All relevant thermodynamic properties at Station 2 are then computed from appropriate calls to REFPROP, (*i.e.,* $\rho_2 = \rho(P_{ATM}, h_2)$, $T_2 = T(P_{ATM}, h_2)$, $Q_2 = Q(P_{ATM}, h_2)$, *etc.).* The source diameter, D_2, at Station 2 is then computed from Equation (9) and the knowledge that $\dot{m}_1 = \dot{m}_2 = \rho_2 \left(\frac{\pi D_2^2}{4}\right) V_2$. The length of Zone 1 is assumed to be negligibly small compared to the lengths of the Zones downstream. This assumption is usually justified by the fact that in under expanded jets, the distance between the leak exit plane and the location of the first Mach disk is usually on the order of 10 leak diameters or less for discharges having the pressure ratios considered here, see, *e.g.* [9]; the shock structure related to the supersonic flow and recovery to atmospheric pressure is confined to an area relatively close to the leak.

2.3 Zone 2 – Zone of Initial Entrainment and Heating

The model for Zone 2, the zone of initial entrainment and heating is similar to the model previously described by Winters and Houf [10-11]. Their model was used in describing slow leaks of hydrogen

in which kinetic energy changes were negligible. In the present work we are interested in describing high momentum leaks where kinetic energy may be important and have therefore extended the model to include kinetic energy terms in the energy equation.

The thermodynamics of leaking hydrogen can be complicated considering it is likely to be a two-phase mixture at extremely low temperature. The thermodynamics become more difficult to describe as the exiting hydrogen stream from Zone 1 entrains the surrounding ambient air. Near the exit to Zone 1 any entrained air is likely to condense or even freeze resulting in a mixture that cannot be characterized by currently available equilibrium models. Even a comprehensive thermodynamic model such as REFPROP cannot characterize mixtures in which two or more of the mixture species exist in the liquid phase. To overcome this difficulty, a "plug flow" turbulent entrainment model is used to model the first stage of air entrainment. The following assumptions are used in developing the model for Zone 2, the zone of initial entrainment and heating: (1) the flow stream is turbulent and quasi-steady; (2) radial molecular diffusion is neglected compared to radial turbulent transport and radial turbulent transport is assumed to occur only at the jet periphery such that radial distributions of velocity concentration and enthalpy are uniform at any axial location in the jet (i.e. a plug-flow model is assumed); (3) streamwise turbulent diffusive transport is negligible compared to streamwise convective transport; (4) buoyancy is neglected due to the fact that the zone of initial entrainment and heating is short and the trajectory of the jet is not significantly altered as a result of buoyant forces; (5) pressure is hydrostatic throughout the flow field and the thermodynamic pressure throughout the flow field is one atmosphere; (6) the hydrogen and air are in thermodynamic equilibrium; (8) and changes in potential energy are negligible.

The Zone 2 model is schematically represented in Fig. 3. The figure shows how continuity, momentum and energy are conserved in the zone of initial entrainment and heating. The exit temperature of the zone is an assumed value T_3. The exit temperature is arbitrary but modeling accuracy requires that this temperature be the lowest temperature where the exiting hydrogen-air mixture can exist as a gas (or the lowest temperature where REFPROP can compute the thermodynamic properties of the mixture). Keeping T_3 low will also cause the zone of initial entrainment and heating to be short or even negligible compared to the remaining two downstream zones that make up the leak jet. In the present study a value of 47 K was selected for T_3 since it was the lowest temperature for which REFPROP could characterize the state for the exiting air-hydrogen mixture.

Figure 4 illustrates the conservation of mass, momentum, and energy for the zone. Pure hydrogen enters the zone on the left (Station 2), air is turbulently entrained at the jet periphery, and an air-hydrogen mixture exits on the right (Station 3). Since the pressure throughout the flow field is uniform and the jet entrains stagnant air, the net pressure forces on the zone are zero and the entering and exit momentum is conserved in the zone resulting in the situation depicted in Fig. 3b. Figure 3c illustrates conservation of energy for the zone. Pure hydrogen enters the zone at the left (Station 2) with a known enthalpy, h_2; air is entrained at the known ambient air enthalpy, h_A and the air-hydrogen mixture exits the right (Station 3) at the enthalpy, h_3. The resulting conservation equations for Zone 2 are:

Mass: $$\dot{m}_2 + \dot{m}_A = \dot{m}_3 \tag{12}$$

Momentum: $$\dot{m}_2 V_2 = \dot{m}_3 V_3 \tag{13}$$

Energy: $$\dot{m}_2\left(h_2 + \frac{1}{2}V_2^2\right) + \dot{m}_A h_A = \dot{m}_3\left(h_3 + \frac{1}{2}V_3^2\right) \tag{14}$$

where V_2 is the velocity of pure hydrogen entering the zone at Station 2 and V_3 is the velocity of the air-hydrogen mixture exiting the zone at Station 3. The value of h_3 is determined from the state

specified by T_3, atmospheric pressure, and the composition of the exiting air-hydrogen mixture. This is accomplished through an appropriate call to REFPROP, i.e.

$$h_3 = h(T_3, P_{ATM}, Y_3) \tag{15}$$

where Y_3 represents the set of mass fractions for exiting air and hydrogen.

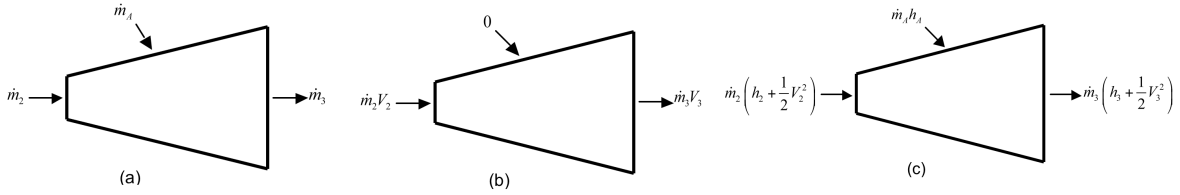

Figure 3. Model for the Zone 2, zone of initial entrainment and heating. (a) Conservation of mass, (b) momentum, and (c) energy.

Equation (12) may be substituted into Eq. (13) to yield the following equation for the velocity at Station 3:

$$V_3 = \frac{\dot{m}_2 V_2}{\dot{m}_2 + \dot{m}_A} \tag{16}$$

Equation (12) may be substituted into Eq. (14) to yield the following energy equation:

$$R = \dot{m}_2\left(h_2 + \frac{1}{2}V_2^2\right) + \dot{m}_A h_A - (\dot{m}_2 + \dot{m}_3)\left(h_3 + \frac{1}{2}V_3^2\right) = 0 \tag{17}$$

The energy Eq. (17) is presented in "residual form" and is satisfied when $R = 0$. Equations (16) and (17) are solved iteratively by successively picking trial values of $\dot{m}_A$ until one is found that sufficiently satisfies Eq. (17). The first trial guess for $\dot{m}_A$ is $\Delta\dot{m}_A$. Subsequent guesses for $\dot{m}_A$ are made by incrementing (increasing) the previous value of $\dot{m}_A$ by $\Delta\dot{m}_A$. As $\Delta\dot{m}_A \to 0$, the procedure yields $R \to 0$ when converged, *i.e.* for a sufficiently small $\Delta\dot{m}_A$, the energy equation is satisfied within acceptable tolerance. During the iteration process the respective mass fractions for hydrogen and air at Station 3 are evaluated from expressions of the form

$$Y_3^{H_2} = \frac{\dot{m}_2}{\dot{m}_2 + \dot{m}_A} \tag{18}$$

$$Y_3^{A} = \frac{\dot{m}_A}{\dot{m}_2 + \dot{m}_A} \tag{19}$$

For cases where the temperature of hydrogen at Station 2 exceeds 47 K, there is no need to make calculations for Zone 2. This is typically true for most gaseous hydrogen leaks in which condensation (formation of a liquid phase) does not occur. In such cases the transition to Station 3 is trivial, with $\dot{m}_3 = \dot{m}_2$, $P_3 = P_2 = P_{ATM}$, $T_3 = T_2$, $V_3 = V_2$, and $D_3 = D_2$.

2.4 Zones 3 & 4 – Zone developing and fully developed flow

The modeling techniques outlined here for Zones 3 and 4 have been developed by Gebhart *et al.* [12] and many others. Winters and Houf [10-11] used these techniques to describe hydrogen dilution for slow leaks. Here we extend the model for high momentum leaks by including kinetic energy in the energy equation.

The assumptions used for Zones 3 & 4 are similar to those stated for Zone 2 except that the influence of buoyancy is included in determining the trajectory of the jet or plume. The flow is no longer a "plug flow" and radial variations of flow properties are permitted. Zone 3 is a relatively short zone in which the leak jet makes the transition from plug flow to fully developed flow. Most of the discussion here relates to Zone 4, the zone of fully developed flow, since this is by far the largest zone in the leak model.

The coordinate system used to describe jet trajectory and growth of the jet is shown in Fig. 2. The jet axis lies along the streamwise coordinate s. The jet radial coordinate is r and the jet circumferential coordinate is ϕ. The angle between the jet axis and the x-axis in the superimposed x-y-z Cartesian coordinate frame of Fig. 2 is θ. The jet is assumed to be symmetrical about the x-y plane, hence the relationship between s, θ, x and y are given by:

$$\frac{dx}{ds} = \cos\theta \tag{20}$$

$$\frac{dy}{ds} = \sin\theta . \tag{21}$$

The integral equations for jet continuity, the two components of momentum, hydrogen concentration, and energy are summarized as follows:

(continuity) $$\frac{\partial}{\partial s}\int_0^{2\pi}\int_0^{\infty}\rho V r dr d\phi = \rho_A E \tag{22}$$

(x-momentum) $$\frac{\partial}{\partial s}\int_0^{2\pi}\int_0^{\infty}\rho V^2 \cos\theta r dr d\phi = 0 \tag{23}$$

(y-momenturm) $$\frac{\partial}{\partial s}\int_0^{2\pi}\int_0^{\infty}\rho V^2 \sin\theta r dr d\phi = \int_0^{2\pi}\int_0^{\infty}(\rho_A - \rho) g r dr d\phi \tag{24}$$

(concentration) $$\frac{\partial}{\partial s}\int_0^{2\pi}\int_0^{\infty}\rho V Y r dr d\phi = 0 \tag{25}$$

(energy) $$\frac{\partial}{\partial s}\int_0^{2\pi}\int_0^{\infty} V\rho\left(h + \frac{1}{2}V^2 - h_A\right) r dr d\phi = 0 \tag{26}$$

where ρ, ρ_A, *V, h, Y, g,* and h_A are the jet density, the density of ambient air, jet velocity, jet enthalpy, jet hydrogen mass fraction, gravitational constant and ambient air enthalpy respectively.

A number of investigators including Albertson *et al.* [13] and more recently Houf and Schefer [14] have shown that within the zone of established flow (Zone 4), the mean velocity profiles are nearly Gaussian and take the form

$$V = V_{CL}\exp(-r^2 / B^2) \tag{27}$$

where V_{CL} is the local centerline velocity, r is the radial coordinate and B is the characteristic jet width or the radial distance at which *V* is equal to *1/e* times V_{CL}. Fan [15], Houlf *et al.* [16] and others have shown that scalar profiles within the jet are also Gaussian and can be expressed as:

$$\rho - \rho_A = (\rho_{CL} - \rho_A)\exp\left(\frac{-r^2}{\lambda^2 B^2}\right) \tag{28}$$

$$\rho Y = \rho_{CL} Y_{CL} \exp\left(\frac{-r^2}{\lambda^2 B^2}\right) \tag{29}$$

where ρ_{CL}, Y_{CL} are the local centerline density and hydrogen mass fraction respectively. The parameter λ represents the relative spreading ratio between velocity and scalar properties ρ , *Y*, and *h* and is related to turbulent entrainment Prandtl and Schmidt number.

The selection of a radial profile for *h* must be constrained in such a way as to satisfy the equation of state for the hydrogen air mixture. If reference enthalpies for each component are assigned a value zero at a temperature of zero, it follows that

$$h = C_p T \tag{30}$$

where C_p is the mixture specific heat. Here we assume the hydrogen-air mixture behaves as a calorically perfect ideal gas (specific heats of air and hydrogen have a negligible variation due to temperature). For a mixture of ideal gases it follows that

$$T = \frac{P_{ATM} M}{\rho \bar{R}} \tag{31}$$

where *M* is the mixture molecular weight and $\bar{R}$ is the universal gas constant. Substituting Eq. (31) into Eq. (33) yields

$$h = \frac{C_p P_{ATM} M}{\rho \bar{R}}. \tag{32}$$

The mixture specific heat and molecular weight can be expressed as

$$C_p = Y C_{p_{H_2}} + (1 - Y) C_{p_A} \tag{33}$$

$$M = \left[\frac{Y}{M_{H_2}} + \frac{1 - Y}{M_A}\right]^{-1} \tag{34}$$

where $C_{p_{H_2}}$ and C_{p_A} are the specific heats of hydrogen and air and M_{H_2} and M_A are the molecular weights. The radial distribution in *h* can be determined by combining Eqs. (28-29), (26), and (32-34). This complicated expression is represented here as

$$h = f(\rho_{CL}, Y_{CL}, B, r). \tag{35}$$

Since the jet is assumed to be axisymmetric, there are no variations in ϕ and the Gaussian profiles given by Eqs. (27-29) may be substituted into the integral Eqs. (22-26) and integrated to yield the following ordinary differential equations:

(continuity)
$$\frac{d}{ds}\left\{V_{CL} B^2 \left[\rho_A - \frac{\lambda_\rho^2}{\left(\lambda_\rho^2 + 1\right)}\left(\rho_A - \rho_{CL}\right)\right]\right\} = \frac{\rho_A E}{\pi} \tag{36}$$

(x-mom.)
$$\frac{d}{ds}\left\{V_{CL}^2 B^2 \cos\theta \left[\rho_A - \frac{2\lambda_\rho^2}{\left(2\lambda_\rho^2 + 1\right)}\left(\rho_A - \rho_{CL}\right)\right]\right\} = 0 \tag{37}$$

(y-mom.) $$\frac{d}{ds}\left\{V_{CL}^2 B^2 \sin\theta\left[\frac{\rho_A}{2}-\frac{\lambda_\rho^2}{\left(2\lambda_\rho^2+1\right)}\left(\rho_A-\rho_{CL}\right)\right]\right\}=\left(\rho_A-\rho_{CL}\right)\lambda_\rho^2 B^2 g \tag{38}$$

(concentration) $$\frac{d}{ds}\left[V_{CL}B^2\left(\rho_A-\rho_{CL}Y_{CL}\right)\right]=0 \tag{39}$$

The energy Eq. (29) reduces to

(energy) $$\frac{\partial}{\partial s}\left\{2\pi\int_0^\infty V\rho(h+\frac{1}{2}V^2-h_{amb})rdr\right\}=0\,. \tag{40}$$

In Eq. (40), V, ρ, and *Y*, are replaced by their Guassian profiles from Eqs. (27), (28) and (29) respectively. Equations (20-21), (36-40), represent a system of 7 ordinary differential equations and algebraic equations with 7 unknowns (x, y, θ, B, ρ_{CL}, V_{CL}, and Y_{CL}). The differential-algebraic solver DDASKR [18] was used to solve these equations. The integral in Eq. (40) is numerically integrated using the trapezoidal rule. Typically, the upper integration limit ∞ is replaced by 3B and 1000 equally spaced intervals are used to perform the integration. Numerical experiments were conducted in which the upper limit of integration was increased to 5B and 10,000 equally spaced intervals were used. The computed values for the seven dependent variables were unaffected in the first four significant figures.

A model for Zone 3, the zone of flow establishment, was used to compute the initial values of the dependent variables (e.g. initial centerline values for density, velocity, mass fraction, enthalpy, etc.) at Station 4. This model was originally proposed by Gebhart et al. [12] and Abraham [19]. Detailed documentation is provided in reference [17].

In order to complete the Gaussian turbulent entrainment model, a model for the entrainment, E in Eq.(36) must be proposed. In the absence of data for the entrainment of air into cold hydrogen jets, the entrainment model of Houf and Schefer [14] was utilized. This entrainment model is based on an approach suggested by Hirst [20]. The Houf and Schefer entrainment model has been experimentally verified for hydrogen jets at ambient temperature. References [14, 17] contain a detailed description of the entrainment model.

3.0 VALIDATION OF THE MODEL FOR GASEOUS HYDROGEN LEAKS

Xiao et al. [7] measured hydrogen concentration along the centerline of four high momentum gaseous hydrogen leak jets. Reservoir conditions and leak diameters for the experiments are summarized in Table 1. To the authors' knowledge, Cases 3 and 4 are the only available measurements for cold hydrogen jet concentration.

Table 1. Reservoir conditions and leak diameter for the experiments of Xiao et al. [7].

Case	Reservoir Pressure P_0 - MPa	Reservoir Temperature T_0 - K	Leak Diameter D_1 - mm
1	1.7	298	2
2	6.85	298	1
3	0.825	80	2
4	3.2	80	1

Each of the leaks in Table 1 was simulated using the multi-stage model documented in the previous sections. In all cases the hydrogen temperature exiting Zone 1 was high enough to permit the air-hydrogen mixture to be treated as an ideal gas. Hence it was not necessary to utilize the model for Zone 2, the zone of initial entrainment and heating and the conditions at Station 3 were instead equated to those at Station 2. The resulting predictions for jet centerline concentration are compared

to the measurements of Xiao *et al*. in Fig. 4. The reciprocal of hydrogen mole fraction is plotted against the normalized axial coordinate. The normalizing factor used was the leak diameter, D_1. Xiao *et al*. utilized a virtual origin, S_1 to display their data. This origin is intended to account for the shock structure upstream of the point where the Gaussian Turbulent entrainment model (Zone 4 and 5) is applied. Xiao *et al*. conclude that the virtual origin displacements were very small (15-30 leak diameters) but did not publish their assumed values. The influence of a virtual origin was ignored for the purposes of displaying the predicted centerline concentrations in Fig. 4.

Predicted hydrogen concentrations compare favorably with measurements for all the four cases. With the exception of Case 1, the model predicts slightly longer values of S for a given hydrogen concentration. Hence the model can be expected to error on the conservative side when it is used to predict hydrogen dilution distances.

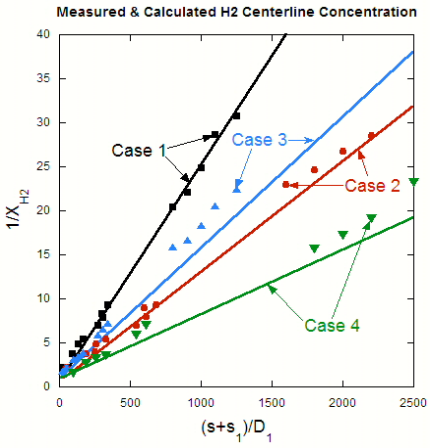

Figure 4. Comparison of model simulations for hydrogen mole fraction along jet centerline with the data from Xiao et al. [7].

4.0 DILUTION DISTANCES FOR MULTI-PHASE HYDROGEN RELEASES

The leak jet model was used to predict 4% dilution distances for three kinds of multi-phase hydrogen leaks originating from a liquid hydrogen storage space. The 4% dilution distance is the distance from the leak location to a location where the centerline concentration (mole fraction or concentration by volume) drops to 4%. The 4% concentration limit is often referred to the lower flammable limit for hydrogen in air.

In all cases the liquid hydrogen storage pressure was assumed to be 1.03 MPa (150 PSI) gage pressure. Leaks were assumed to emanate from three different storage locations: (1) the saturated vapor storage space, (2) the saturated liquid storage space, or (3) a subcooled liquid storage space.

The subcooled liquid calculations were an attempt to simulate leaks from a storage system shortly after a tanker truck replenished the supply of liquid hydrogen. For these calculations the state of the hydrogen at Station 0 was assumed to be specified by the storage pressure 1.03 MPa (150 PSIG) and the density of saturated liquid at 0.207 MPa (30 PSIG), or 65 kg/m^3.

All simulated multi-phase hydrogen leaks resulted in a source of atmospheric hydrogen near or below the hydrogen critical temperature (33.145 K), i.e. the state of hydrogen at Station 2 (exit plane for Zone 1, the zone of under expanded flow) was cold enough to condense or even solidify air. As a result the model for Zone 2, the zone of initial entrainment and heating, was required to bring the air-hydrogen mixture to a state where the pressure and temperature was 1 atmosphere and 47 K respectively. The resulting velocity, V_3 and flow diameter, D_3 were then used as starting conditions in the Gaussian turbulent entrainment calculations (i.e. Zones, 3 and 4). In all cases the computed length of Zone 2 was found to be negligible compared to the computed 4% dilution distances. The

entrainment model of Houf and Schefer [14] was used to compute the Zone 2 length for these comparisons.

The computed 4% dilution distances for the three types of multi-phase hydrogen leaks are shown in Table 2. Leaks were assumed to occur from pipes ID's ranging in diameter from 6.35 mm (¼ in) to 50.8 mm (2 in). These diameters are shown in column one of each leak table. The leak diameter used for each pipe size was based on using a leak flow area of 3% of the pipe flow area. These diameters are shown in column two of each table. The use of 3% of pipe flow area leaks is based on the leak size used in the risk-informed gaseous hydrogen separation distance work performed by NFPA 2 Task Group 6 and documented in LaChance et al. [21]. The computed 4% dilution distances are shown in column three of each table.

Table 2. Dilution distance to 4% hydrogen mole fraction concentration for 3 types of multi-phase hydrogen leaks.

Saturated Vapor Leak[1]		
Pipe ID (mm)	Leak Diameter[4] (mm)	Distance[5] (m)
6.35 mm (1/4 in)	1.100	4.431
12.7 mm (1/2 in)	2.200	8.861
19.05 mm (3/4 in)	3.299	13.29
25.4 mm (1 in)	4.399	17.71
31.75 mm (1.25 in)	5.499	22.13
38.10 mm (1.5 in)	6.599	26.55
44.45 mm (1.75 in)	7.699	30.96
50.80 mm (2 in)	8.799	35.36

Saturated Liquid Leak[2]		
Pipe ID (mm)	Leak Diameter[4] (mm)	Distance[5] (m)
6.35 mm (1/4 in)	1.100	5.659
12.7 mm (1/2 in)	2.200	11.26
19.05 mm (3/4 in)	3.299	16.75
25.4 mm (1 in)	4.399	22.11
31.75 mm (1.25 in)	5.499	27.31
38.10 mm (1.5 in)	6.599	32.37
44.45 mm (1.75 in)	7.699	37.29
50.80 mm (2 in)	8.799	42.06

Subcooled Liquid Leak[3]		
Pipe ID (mm)	Leak Diameter[4] (mm)	Distance[5] (m)
6.35 mm (1/4 in)	1.100	9.611
12.7 mm (1/2 in)	2.200	15.9
19.05 mm (3/4 in)	3.299	21.94
25.4 mm (1 in)	4.399	27.64
31.75 mm (1.25 in)	5.499	33.09
38.10 mm (1.5 in)	6.599	38.34
44.45 mm (1.75 in)	7.699	43.46
50.80 mm (2 in)	8.799	48.4

1. Leak from saturated vapor space at 1.03 MPa (150 PSIG)
2. Leak from saturated liquid space at 1.03 MPa (150 PSIG)
3. Leak from subcooled liquid at 1.03 MPa (150 PSIG) and density of saturated liquid (65 kg/m3) at 0.207 MPa (30 PSIG)
4. Diameter based on 3% of pipe flow area.
5. Distance to location where hydrogen concentration is 4% by volume

5.0 SUMMARY

A model for computing hydrogen dilution distances from liquid hydrogen storage spaces has been presented. The model has been validated against experimental data presented by Xiao et al. [7] for leaks of room temperature hydrogen and 80 K high-pressure hydrogen gas. The model has been used to simulate jet dilution distances to the lower flammability limit of hydrogen (4% mole fraction) in under-expanded high-pressure leaks from the saturated vapor space and the saturated liquid space of a liquid hydrogen storage tank at 1.03MPa (150 psig). Simulations were also performed for a subcooled liquid leak from the same tank for conditions that represent the recent replenishment of the liquid hydrogen by a tanker truck.

The simulations showed that the dilution distances for the saturated vapor leaks were the shortest of the three multi-phase leaks considered; leaks from the saturated liquid space were approximately 19-28% longer than the corresponding leaks from the saturated vapor space. The largest dilution distances computed were for subcooled liquid leaks. These leaks were approximately 37-117% longer than the corresponding saturated vapor leaks. The calculated results reflect the fact that saturated liquid and subcooled liquid leaks enter the atmosphere as two-phase mixtures having higher qualities (denser hydrogen streams) than saturated vapor leaks. As a result, longer distances are required to entrain sufficient air to dilute these leaks. Furthermore, these leaks are negatively buoyant in air while all saturated vapor leaks are positively buoyant. It should be pointed out that since these are high-momentum releases, the trajectory of leaks to their 4% dilution distances were not influenced greatly by buoyancy.

ACKNOWLEDGEMENTS

This work was supported by the U.S. Department of Energy, Office of Energy Efficiency and Renewable Energy, Fuel Cell Technologies Program under the Safety, Codes, and Standards subprogram element managed by Antonio Ruiz.

REFERENCES

1. Lemmon, E. W., Huber, M. L., McLinden, M. O., "NIST Reference Fluid Thermodynamic and Transport Properties-REFPROP," Version 8 User's Guide, U. S. Department of Commerce Technology Administration, National Institute of Standards and Technology, Standard Reference Data Program, Gaithersburg, Maryland 20899, April, 2007.
2. Moody, F. J., "Maximum Flow Rate of a Single-Component, Two-Phase Mixture," Trans. of the ASME, Jour. of Heat Transfer, Vol. 87, pp. 134-142, 1965.
3. Henry, R. E. and Fauske, H. K., "The Two-Phase Critical Flow of One-Component Mixtures in Nozzles, Orifices and Short Tube," Trans. of the ASME, Jour. of Heat Transfer, Vol. 93, pp. 179-187, 1985.
4. Jeong, J. J., Ha, K. S., Chung, B. D. and Lahey Jr., R. T., "Development of a Multi-Dimensional Thermal Hydraulic System Code, MARS 1.3.1," Annals of Nuclear Energy, Vol. 26, pp. 1611-1642, 1999.
5. Chung, M. S., Park, S. B., Lee, H. K., "Sound Speed Criterion for Two-Phase Critical Flow," Jour. of Sound and Vibrations, Vol. 276, pp. 13-26, 2004.
6. Birch, A. D., Hughes, D. J., and Swaffield F., "Velocity Decay of High Pressure Jets," Comb. Science and Technology, Vol. 36, 1987.
7. Xiao, J., Travis, J. R., and Breitung, W., "Hydrogen Release from a High Pressure Gaseous Hydrogen Reservoir in Case of a Small Leak," Inter. Jour. of Hydrogen Energy, Vol. 36, No. 3, pp. 2545-2554, 2011.
8. Yuceil, K. B. and Ottugen, M. V.," Scaling Parameters for Underexpanded Supersonic Jets," Physics of Fluids, Vol. 4, No. 12, pp. 4206-4215, 2002.
9. Crist, S., Sherman, P. M., and Glass, R. R, "Study of the Highly Underexpanded Sonic Jet," AIAA Journal, Vol. 4, No. 1, 1966.
10. Winters, W. S., and Houf, W. G., "Simulation of Small-Scale Releases from Liquid Hydrogen Storage Systems," Inter. Jour. of Hydrogen Energy, Vol. 36, No. 6, pp. 3913-3921, 2011.
11. Winters, W. S. and Houf, W. G., "Simulation of Small-Scale Releases from Liquid Hydrogen Storage Systems," Proceedings of the 3rd International Conference on Hydrogen Safety, Ajaccio-Corsica, France, September 16-18, 2009.
12. Gebhart, B., Hilder, D. S., and Kelleher, M., "The Diffusion of Turbulent Buoyant Jets," Adv. in Heat Transfer, Vol. 16, Academic Press, Inc., Orlando, Florida, 1984.
13. Albertson, M. L., Dai, Y. B., Jensen, R. A., and Rouse, H., "Diffusion of Submerged Jets," Trans. of the Amer. Society of Civil Eng., Vol. 115, pp. 639-697, 1950.
14. Houf, W. and Schefer, R., "Analytical and Experimental Investigation of Small-Scale Unintended Releases of Hydrogen," Inter. Jour. of Hydrogen Energy, Vol. 33, No. 4, pp. 1435-1444, 2008.
15. Fan, L. H., "Turbulent Buoyant Jets into Stratified and Flowing Ambient Fluids," Rep. No. KH-R-15, W. M. Keck Laboratory, California Institute of Technology, Pasadena, 1967.
16. Hoult, D. P., Fay, J. A., and Forney, L. J., "A Theory of Plume Rise Compared with Field Observations," Journal of Air Pollution Control Assoc., Vol. 19, 585-590, 1969.
17. Winters, W. S., "Modeling Leaks from Liquid Hydrogen Storage Systems," SAND2009-0035, Sandia National Laboratories, Livermore, CA, January, 2009.
18. Petzold, L. R., Brown, P. N., Hindmarsh, A. C., and Ulrich, C. W., "DDASKR – Differential Algebraic Solver Software," Center for Computational Science & Engineering, L-316, Lawrence Livermore National Laboratory, P.O. Box 808, a private communication with L. R. Petzold.
19. Abraham, G., "Horizontal Jets in Stagnant Fluid of Other Density," Journal Hydraul. Div. Am. Soc. Civ. Eng., Vol. 9, 1965.
20. Hirst, E. A., "Analysis of Buoyant Jets within the Zone of Flow Establishment," Oak Ridge National Laboratory Report, ORNL-TM-3470, 1971.
21. LaChance, J., Houf, W., Middleton, B., Fluer, L., "Analysis to Support Development of Risk-Informed Separation Distances for Hydrogen Codes and Standards," Sandia Report SAND2009-0874, March 2009.